Ground states of group-IV nanostructures: Magic structures of diamond and silicon nanocrystals

Xiaobao Yang* and Yu-Jun Zhao
Department of Physics, South China University of Technology, Guangzhou 510640, People's Republic of China

Hu Xu
Department of Physics and Materials Science, City University of Hong Kong, Hong Kong SAR, China

Boris I. Yakobson†
Department of Mechanical Engineering and Materials Science, Department of Chemistry, The Richard E. Smalley Institute for Nanoscale Science and Technology, Rice University, Houston, Texas 77005, USA

(Received 6 April 2011; published 23 May 2011)

We have developed an effective model to investigate the energetic stability of hydrogenated group-IV nanostructures, followed by validations from density-functional theory calculations. The Hamiltonian of X_mH_n (X = C, Si, Ge, and Sn) is expressed analytically by the atom numbers (m, n) and the magic numbers of diamond nanocrystals and silicon nanocrystals are determined. It is found that surface reconstructions would alter the morphology of silicon nanocrystals significantly and consequently induce dramatic modulation on their electronic properties.

DOI: 10.1103/PhysRevB.83.205314 PACS number(s): 61.46.Df, 68.65.−k

I. INTRODUCTION

Semiconductor nanocrystals (NCs) have been greatly attractive and intensively investigated.[1,2] These nanomaterials have extended the physics of reduced dimensions and offered the opportunity for fundamental study of the regime between nanostructure and bulk states,[3] which have also brought such wide applications as nanoscale electronic and optical devices,[4] fluorescent biological labels,[5] quantum computation media,[6] etc.

Various hydrogenated group-IV [C,[7,8] Si,[9,10] and Ge (Ref. 11)] nanocrystals with sp^3 hybridizations have been synthesized and isolated, in which size-dependent optical gaps have been observed. To demonstrate the quantum confinement, theoretical studies have focused on the optical properties of nanocrystals[12,13] and employed various methods for accurate calculations of the adsorption spectrum.[14,15] However, surface reconstruction is predicted to be energetically preferable, which would dramatically reduce the optical gaps and decrease excitonic lifetimes.[16] Meanwhile, the spatial charge distributions of the highest occupied and the lowest unoccupied states are also crucial in the design of the optical nanodevice.[17]

Properties of nanomaterials mostly depend on their structures, however, it is challenging to determine the stable nanostructures from numerous possible candidates due to two main obstacles: (i) the accurate calculation of the total energy is necessary but often computationally expensive, and (ii) many isomeric structures should be considered and the number of these structures increases sharply as the size increases. To reduce the time cost, recent studies[18,19] calculated the energies using classical potential in Hansel-Vogel (HV) formalism, and searched the magic structures of silicon nanowires using genetic algorithms. The energy decomposition approach[20,21] is also efficient for stability investigations, where the total energy is separated into contributions from the bulk, surfaces, and the edges between the facets. It is shown that the ground state of thinnest silicon nanowire is of a five-fold rather than a single-crystal type,[20] which is in agreement with experimental observations.[22]

In this paper, we investigate hydrogenated group-IV nanocrystals by both model analysis and first-principles approaches. We propose an effective model and give an analytical expression of the Hamiltonian for X_mH_n (X = C, Si, Ge, and Sn) with the numbers of atoms (m,n), as is confirmed by density-functional theory (DFT) calculations. Magic numbers of diamond nanocrystals obtained in our searches are consistent with the experimental results. We also predict stable Si NCs with unique electronic properties.

II. MODEL ANALYSIS

In this section, we study the stability of hydrogenated group-IV nanocrystals X_mH_n, according to the effective model of Hamiltonian. We find that there is an analytical dependence of total energies on the numbers of atoms (m,n), which greatly enhances the searching efficiency of stable nanostructures. We obtain possible stable structures with the stochastic technique and determine the ground-state structures by the simplex method.

A. The effective Hamiltonian model

In our model, we assume the Hamiltonian of X_mH_n (X = C, Si, Ge, and Sn) to be

$$\mathcal{H} = \sum_{i=1}^{m} \left(\mathcal{H}^i_{\text{int}} + \mathcal{H}^i_0\right) - m\mu_X - n\mu_{\text{H}} \qquad (1)$$

where $\mathcal{H}^i_{\text{int}}$ and $\mathcal{H}^i_0$ are the contributions from interactions and self energies, and $\mu_X(\mu_{\text{H}})$ is the chemical potential for X(H) atom. The sum runs over all the group-IV atoms and we have $\mathcal{H}^i_0 = \mu_{X_0} + p_i\mu_{\text{H}_0}$, where p_i is the number of H atoms in the saturated group of the ith X atom and $\mu_{X_0}(\mu_{\text{H}_0})$ is the isolated atomic energy for the X(H) atom. $\mathcal{H}^i_{\text{int}}$ includes the energy contributions from the bonded X-atom pair ($-E_{X\text{-}X}$)

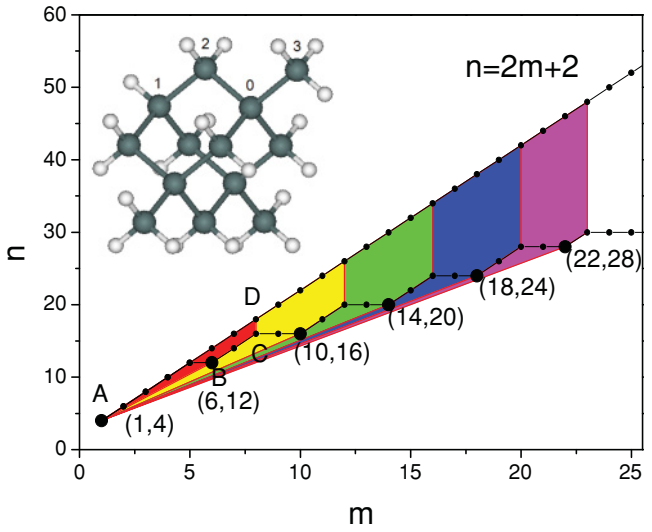

FIG. 1. (Color online) Possible (m, n) for X_mH_n. The convex corresponds to the local minimum and stable structures of hydrogenated nanostructures. Light and dark balls represent H and X atoms, respectively.

and the saturated group of the ith X atom $(-E_{-XH_{p_i}})$. As shown in the inset of Fig. 1, every X atom has four nearest neighbors and every X-X bond is shared by two X atoms. This leads the energy contribution corresponding to the ith X atom to be $-2E_{X\text{-}X}$ for $p_i = 0$, and $-1.5E_{X\text{-}X} - E_{X\text{-}H}$ for $p_i = 1$, analogically. Thus, $\mathcal{H}^i_{\text{int}} = -(2 - 0.5p_i)E_{X\text{-}X} - E_{-XH_{p_i}}$. We assume that the interaction between X and H atoms is localized and thus $E_{-XH_{p_i}} = p_i E_{X\text{-}H}$, $p_i = 0,1,2,3$. With $n = \sum_{i=1}^{m} p_i$, we found that Eq. (1) can be written as $\mathcal{H} = am + bn$, where $a = (-2E_{X\text{-}X} - \mu_X + \mu_{X_0})$ and $b = (E_{X\text{-}H} + 0.5E_{X\text{-}X} - \mu_H + \mu_{H_0})$, where μ_X and μ_H are the environment-related parameters, while $E_{X\text{-}X}(E_{X\text{-}H})$ and $\mu_{X_0}(\mu_{H_0})$ can be derived from first-principles calculations or experimental data.

B. Determination of ground-state structures by the simplex method

Instead of scanning the parameter space (a, b),[23] the simplex method[24–26] is used to efficiently determine the combinations of lowest energy from a set of possible integer combinations (m,n), which indicates that the stable configurations correspond to corners, edges, and faces.[26] We will obtain the ground states if we construct enough restricting inequalities and solve the corresponding linear equations.[26] In our case, we have $m \geqslant 1$ and $n \leqslant 2m + 2$. The key task is to determine the lower limit of n for a certain m, for which it is difficult to find out the expected inequalities. We search the least n as follows:[27] (i) start from an arbitrary configuration of X_mH_n $(n \leqslant 2m + 2)$, allowing X atoms on the surface to walk randomly in the crystal lattice and saturate the configuration with H atoms where necessary, and (ii) accept the new configuration when the H-atom number is nonincreasing, otherwise the new geometry will be accepted with the probability of $1/|dn|$, where dn is the increment of the H-atom number. n converges into the minimum after hundreds of iterations.

Figure 1 shows the upper and lower limit of n as a function of m. It is not a standard simplex because both m and n will be increasing with an increasing nanocrystal size of X_mH_n. However, we will obtain a convex quadrangle $\mathcal{ABCD}$ if a restriction of $m \leqslant 8$ is considered. The convex $\mathcal{A}$ (1, 4) and $\mathcal{B}$ (6, 12) correspond to stable configurations, while $\mathcal{C}$ (8, 16) and $\mathcal{D}$ (8, 18) do not since they are induced by the artificial restriction of $m \leqslant 8$. Thus, XH_4 and X_6H_{12} will be stable configurations for group-IV nanocrystals. Analogically, we will obtain a new convex quadrangle (in red and yellow) and find another stable configuration of $X_{10}H_{16}$ in place of X_6H_{12} if we consider a restriction of $m \leqslant 12$. In addition, we find that $X_{14}H_{20}$, $X_{18}H_{24}$, and $X_{22}H_{28}$ are also stable configurations. It should be noted that, except for XH_4, all other nanocrystals are metastable states since they are local-convex ascribed to the size confinement. As is known, the size of nanocrystals increases with increasing reaction time as more material is added to the surfaces.

In general, the total energies (E_{tot}) obtained by DFT do not involve the environment-related chemical potentials and correspond to the Hamiltonian in Eq. (1) with $\mu_X = \mu_H = 0$. Thus, we have $E_{\text{tot}} = a_0 m + b_0 n$, where $a_0 = (-2E_{X\text{-}X} + \mu_{X_0})$ and $b_0 = (-E_{X\text{-}H} + 0.5E_{X\text{-}X} + \mu_{H_0})$. According to our model, we conclude that: (i) E_{tot} can be estimated in the analytical expression of (m,n), which indicates the fast calculation of total energies; (ii) only a few possible candidates of X_mH_n should be considered, as isomeric structures with the same composition will possess the same E_{tot}; and (iii) magic numbers of X_mH_n correspond to the candidates with the most or least n for a certain m, which have been found by our iterations. In the searching process of magic numbers, we obtained different stable structures with the same composition, because the new configuration is accepted when the H atom number is nonincreasing. Interestingly, there are few isomeric structures for candidates with magic numbers and the structure is unique for X_6H_{12}, $X_{10}H_{16}$, and $X_{14}H_{20}$.

III. FIRST-PRINCIPLES CALCULATIONS

In this section, we investigate hydrogenated group-IV nanocrystals X_mH_n with first-principles approaches. We first verify our model by the dependence of E_{tot} on the numbers of atoms (m,n), together with the linear relationship of cohesive energy on the ratio (n/m). According to the phase diagram of chemical potential, we determine the stable structures of diamond NCs, in excellent agreement with the experimental observations. For Si NCs, we find that surface reconstructions would enhance the stability and also induce significant modulation on the electronic properties, such as the gap values and charge distributions of the highest-occupied molecular orbitals (HOMOs) and lowest-unoccupied molecular orbitals (LUMOs).

A. Model verification

To verify the reliability of our model, we investigate the energetic stability of group-IV nanocrystals (with the example of diamond NCs and Si NCs), using the DFT method implemented in the Vienna *Ab initio* Simulation Package (VASP).[28,29] We use Vanderbilt ultrasoft pseudopotentials[30] and the exchange correlation with the generalized gradient

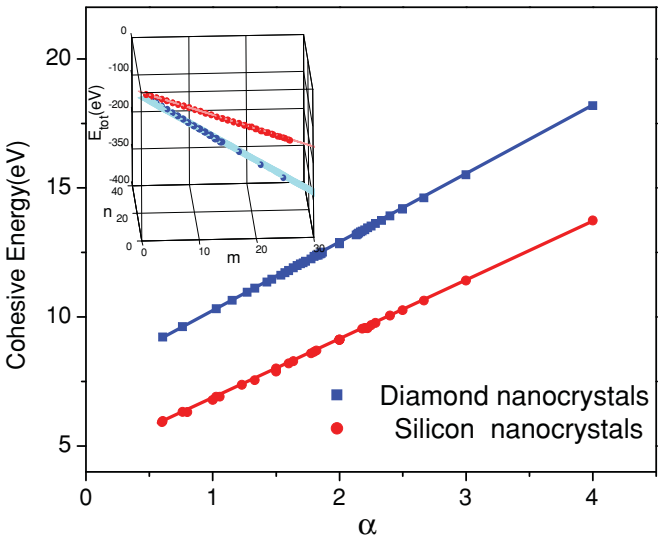

FIG. 2. (Color online) Cohesive energies of diamond NCs and Si NCs as a function of α. Inset shows the dependence of $E_{\rm tot}$ on (m, n). The dots are obtained from the first-principles calculations.

approximation given by Perdew and Wang.[31] We set the plane-wave cutoff energy to be 350 eV and the convergence of the force on each atom to be less than 0.01 eV/Å. A $1 \times 1 \times 1$ mesh of **k** space is used and the vacuum distance is 9 Å, which is enough to make the systems isolated.

As shown in Fig. 2 (inset), the dots of (m,n, $E_{\rm tot}$) for diamond NCs and Si NCs satisfy the plane equations respectively, which confirms the model result of $E_{\rm tot} = a_0 m + b_0 n$. We define the cohesive energy ($E_{\rm coh}$) per X atom in the nanocrystals $X_m H_n$ as $E_{\rm coh} = (m\mu_{X_0} + n\mu_{\rm H_0} - E_{\rm tot})/m$. According to our model, we have: $E_{\rm coh} = 2E_{X\text{-}X} - (0.5E_{X\text{-}X} - E_{X\text{-H}})\alpha$, where α is the ratio (n/m). As predicted, the cohesive energy decreases with the decrease of α following a linear relationship (shown in Fig. 2) approaching the value of bulk material ($-\mu_{\rm diamond\ bulk} = 7.65$ eV and $-\mu_{\rm Si\ bulk} = 4.67$ eV) when α reaches zero.[32]

B. Stable structures of diamond NCs

In the following, we investigate the stable structures of diamond NCs ($C_m H_n$). We calculated $E_{\rm tot}$ of $C_m H_n$ with $m \leqslant 12$ by DFT and obtained the formation energies as a function of hydrogen chemical potential by $E_f = (E_{\rm tot} - m\mu_{X_0} - n\mu_{\rm H_0} - n\mu_{\rm H})/m$. As shown in the inset of Fig. 3, we find that there is a critical point μ_0 (about -2.6 eV, our model indicates $\mu_0 = 0.5E_{\rm C-C} - E_{\rm C-H} \simeq -2.63$eV) of chemical potential, at which the formation energies are the same for all these nanocrystals. Below the critical point $C_{10}H_{16}$ is the most stable, while CH_4 is the most stable when $\mu_{\rm H}$ is above the critical point. As predicted, CH_4 and $C_{10}H_{16}$ are stable states when the number of carbon atoms $m \leqslant 12$. It should be noted that there is certain difference in $E_{\rm tot}$ of isomeric structures obtained from the DFT, while our model indicates $E_{\rm tot}$ would be the same. However, the corresponding E_f is similar for isomeric structures, especially for $\mu_{\rm H}$ far away from the critical point. We can consider only one structure for each composition to enhance the efficiency, as is predicted in our model.

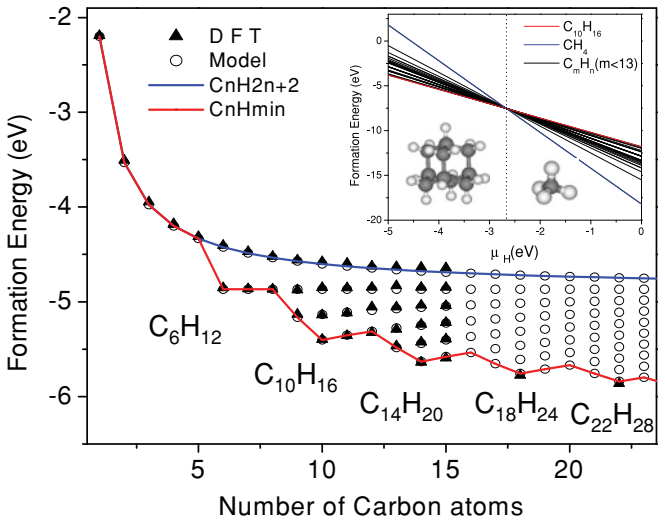

FIG. 3. (Color online) Formation energies as a function of the number of carbon atoms for diamond NCs with $\mu_{\rm H} = -4$ eV. Inset shows the chemical phase diagram for $C_m H_n$ with $m \leqslant 12$. Light and dark balls represent H and C atoms, respectively.

Figure 3 shows the formation energies for various $C_m H_n$ with the chemical potential of hydrogen $\mu_{\rm H} = -4$ eV. The hollow circles are from our model prediction, which is in excellent agreement with the ones from the DFT calculations (marked with solid triangles). For a certain m, the formation energy decreases as the hydrogen atom number n decreases. The stable structures can be found at the local minimum of the formation energies, such as $C_{10}H_{16}$, $C_{14}H_{20}$, $C_{18}H_{24}$, and $C_{22}H_{28}$, which are consistent with our model analysis and experimental observations.[7,8] We can also conclude that, for the chemical potential $\mu_{\rm H} > \mu_0$, the formation energy will

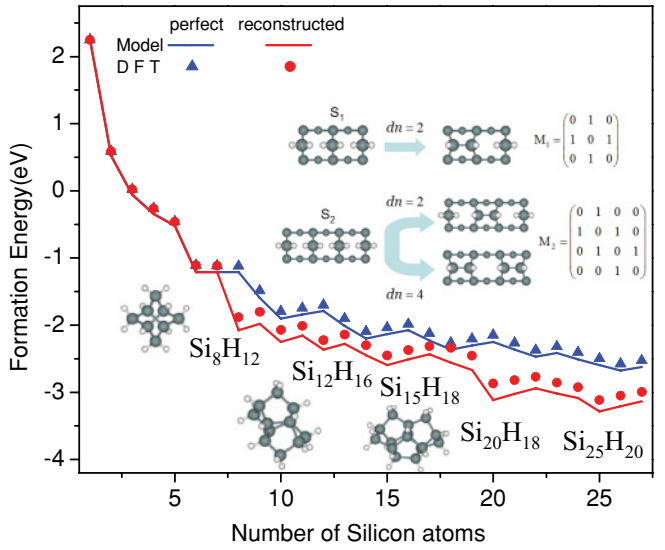

FIG. 4. (Color online) Formation energies as a function of the number of silicon atoms for Si NCs with and without the dimer reconstructions. Inset shows the possible dimer reconstructions and their effect on the number of hydrogen atoms. Light and dark balls represent H and Si atoms, and the size of dark balls corresponds to Si atoms on different layer.

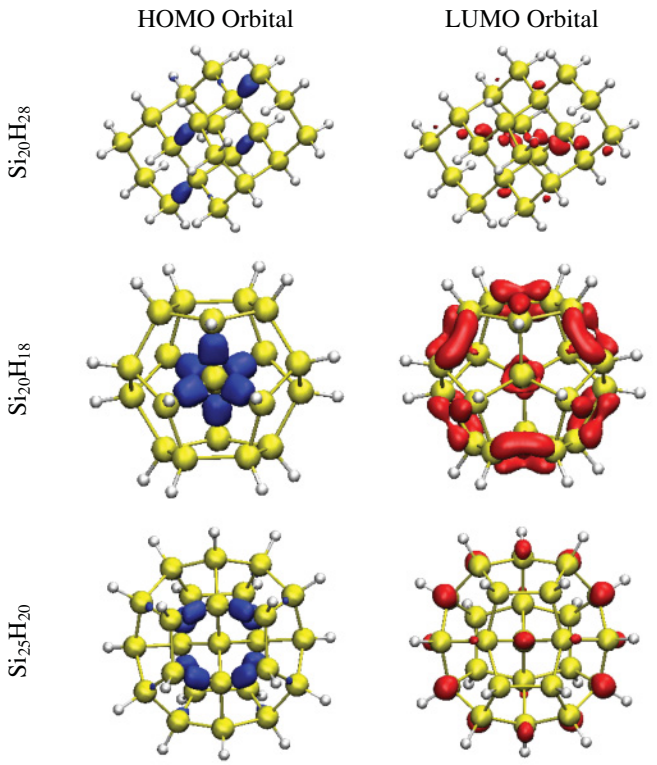

FIG. 5. (Color online) Charge distribution of HOMO and LUMO orbital of $Si_{20}H_{32}$, $Si_{20}H_{18}$, and $Si_{25}H_{20}$. Charge density isosurfaces (blue/dark gray and red/gray) represent 50% peak amplitude.

decrease as the hydrogen atom number n increases for a certain m, thus the stable structures are well-known alkanes C_mH_{2m+2}. It is noted that larger members of diamond NCs obtained experimentally have smaller surface-to-volume ratios and correspondingly lower H/C ratios, though higher diamondoids have been also synthesized and isolated.[7] Our model indicates that diamond NCs with the least H atoms are ground states when $\mu_H < \mu_0$, which correspond to low E_f and thus high thermal stability.

C. Stable structures and electronic properties of Si NCs

Without surface reconstruction, magic numbers of X_mH_n are the same for all group-IV elements (e.g., diamond NCs and Si NCs).[33] In the following, we consider the formation of dimer reconstruction for Si NCs, which is common and often dominates surface reconstruction.[10,16,20] Our DFT calculations showed that the E_{coh} of Si NCs with reconstructions also follow the linear dependence on the H/Si ratio (shown in Fig. 2).

As is shown in Fig. 4, the decrement of H atom number varies with possible reconstructions (e.g., S_1 and S_2). We construct a matrix according to the arrangement of Si atoms with $-SiH_2$: The element $M(i,j)$ in the matrix is 1 when a dimer could be formed by the ith and jth Si atoms, otherwise, it is 0 ($M_1$and M_2 for $S_1$and S_2, respectively). The max decrement of hydrogen atom number is equal to the rank of the matrix.[34] We search the least H number n for Si NCs (Si_mH_n) with a certain m through a similar procedure. With E_{tot} from the DFT, we obtained E_f of Si NCs with and without reconstructions with $\mu_H = -4$ eV. The dimer reconstruction decreases E_f and changes the stable structures. For example, $Si_{10}H_{16}$ might not be the stable structure as E_f is higher than that of Si_8H_{12}, which can be obtained from Si_8H_{16} with two dimer reconstructions. Besides, $Si_{12}H_{16}$, $Si_{15}H_{18}$, $Si_{20}H_{18}$, and $Si_{25}H_{20}$ are new stable structures. The reconstructions also have significant effect on the symmetry of Si NCs. Stable Si NCs without reconstructions tend to be octahedron enclosed by (111) facet (e.g., $Si_{35}H_{36}$). However, the reconstructed $Si_{20}H_{18}$ has the symmetry of C_{3v} and $Si_{25}H_{20}$ is approximately spherical.

Silicon NCs has been an ideal system of demonstrating quantum confinement, as the gap values are inversely proportional to the dot diameter.[12] The gap value of $Si_{20}H_{28}$ (the stable structure for Si NCs without surface reconstructions) is 3.80 eV, and both HOMO and LUMO orbits are concentrated in the central area (shown in Fig. 5). However, surface reconstruction dramatically decreases the gaps and the decrement of value depends on the number of Si atoms. The gap value of $Si_{20}H_{18}$ (2.84 eV) is a local minimum for Si_mH_n with $m \leqslant 26$, while it is 3.19 eV for $Si_{25}H_{20}$ with larger size. It is noted that HOMO orbits are mainly distributed inside while LUMO orbits are concentrated near the surface for $Si_{20}H_{18}$ and $Si_{25}H_{20}$. For LUMO orbits, there is dimerlike distribution for $Si_{20}H_{18}$, while the distribution is localized for $Si_{25}H_{20}$. These nanostructures with spatial separation of orbital distributions might be useful in Si-based laser devices, as they would avoid electron-hole recombination and increase the lifetime of exciton carriers.[17]

IV. SUMMARY

In summary, we have proposed an effective method for the analytical expression of the Hamiltonian of H-terminated group-IV nanostructures, and provided an efficient technique of searching stable structures of X_mH_n (X = C, Si, Ge, and Sn). We showed that the isomeric structures are nearly energetically degenerated and thus the computational cost can be greatly reduced, which is an important complement to the popular DFT calculations for stability determination. The ground-state structure of Si NCs are surface reconstructed, where the highest occupied states are confined in the core and the lowest unoccupied states are distributed on the surface.

ACKNOWLEDGMENTS

This work was supported by the National Natural Science Foundation of China (No. 10704025), the New Century Excellent Talents Program (No. NCET-08-0202) and the Fundamental Research Funds for the Central Universities (No. 2011ZM0090). Work at Rice (B.I.Y.) was supported by the Robert A. Welch Foundation (C-1590).

*scxbyang@scut.edu.cn
†biy@rice.edu

[1] A. P. Alivisatos, J. Phys. Chem. **100**, 13226 (1996).
[2] C. Burda, X. Chen, R. Narayanan, and M. A. EI-Sayed, Chem. Rev. **105**, 1025 (2005).
[3] S. M. Reimann and M. Manninen, Rev. Mod. Phys. **74**, 1283 (2002).

[4]L. Pavesi, L. Dal Negro, C. Mazzoleni, G. Franzo, and F. Priolo, Nature (London) **408**, 440 (2000).
[5]M. Bruchez, M. Moronne, P. Gin, S. Weiss, and A. P. Alivisatos, Science **281**, 2013 (1998).
[6]D. Loss and D. P. DiVincenzo, Phys. Rev. A **57**, 120 (1998).
[7]J. E. Dahl, S. G. Liu, and R. M. K. Carlson, Science **299**, 96 (2003).
[8]L. Landt, K. Klünder, J. E. Dahl, R. M. K. Carlson, T. Möller, and C. Bostedt, Phys. Rev. Lett. **103**, 047402 (2009).
[9]T. van Buuren, L. N. Dinh, L. L. Chase, W. J. Siekhaus, and L. J. Terminello, Phys. Rev. Lett. **80**, 3803 (1998).
[10]G. Belomoin, J. Therrien, A. Smith, S. Rao, R. Twesten, S. Chaieb, M. H. Nayfeh, L. Wagner, and L. Mitas, Appl. Phys. Lett. **80**, 841 (2002).
[11]C. Bostedt, T. van Buuren, T. M. Willey, N. Franco, L. J. Terminello, C. Heske, and T. Möller, Appl. Phys. Lett. **84**, 4056 (2004).
[12]S. Öğüt, J. R. Chelikowsky, and S. G. Louie, Phys. Rev. Lett. **79**, 1770 (1997).
[13]C. S. Garoufalis, A. D. Zdetsis, and S. Grimme, Phys. Rev. Lett. **87**, 276402 (2001).
[14]M. Rohlfing and S. G. Louie, Phys. Rev. Lett. **80**, 3320 (1998).
[15]M. Vörös and A. Gali, Phys. Rev. B **80**, 161411 (2009).
[16]A. Puzder, A. J. Williamson, F. A. Reboredo, and G. Galli, Phys. Rev. Lett. **91**, 157405 (2003).
[17]Z. Wu, J. B. Neaton, and J. C. Grossman, Phys. Rev. Lett. **100**, 246804 (2008).
[18]T. L. Chan, C. V. Ciobanu, F. C. Chuang, N. Lu, C. Z. Wang, and K. M. Ho, Nano Lett. **6**, 277 (2006).
[19]N. Lu, C. V. Ciobanu, T. L. Chan, F. C. Chuang, C. Z. Wang, and K. M. Ho, J. Phys. Chem. C **111**, 7933 (2007).
[20]Y. Zhao and B. I. Yakobson, Phys. Rev. Lett. **91**, 035501 (2003).
[21]N. Gonzalez Szwacki and B. I. Yakobson, Phys. Rev. B **75**, 035406 (2007).
[22]M. Takeguchi, M. Tanaka, H. Yasuda, and K. Furuya, Surf. Sci. **493**, 414 (2001).
[23]X. Yang and J. Ni, Phys. Rev. B **67**, 195403 (2003).
[24]U. Brandt, Z. Phys. B **53**, 283 (1983); U. Brandt and J. Stolze, *ibid.* **62**, 433 (1986); **64**, 481 (1986).
[25]J. Kanamori, Prog. Theor. Phys. **35**, 16 (1966).
[26]J. Stolze, Phys. Rev. Lett. **64**, 970 (1990).
[27]For simplicity, we did not consider any reconstruction.
[28]G. Kresse and J. Hafner, Phys. Rev. B **47**, 558 (1993); **49**, 14251 (1994).
[29]G. Kresse and J. Furthmüller, Comput. Mater. Sci. **6**, 15 (1996); Phys. Rev. B **54**, 11169 (1996).
[30]D. Vanderbilt, Phys. Rev. B **41**, 7892 (1990).
[31]J. P. Perdew, J. A. Chevary, S. H. Vosko, K. A. Jackson, M. R. Pederson, D. J. Singh, and C. Fiolhais, Phys. Rev. B **46**, 6671 (1992).
[32]X. Yang and J. Ni, Phys. Rev. B **72**, 195426 (2005).
[33]H. Xu, X. B. Yang, C. S. Guo, and R. Q. Zhang, Appl. Phys. Lett. **95**, 253106 (2009).
[34]It can be comprehensible that the max decrement of the hydrogen number is independent of the order of Si atoms, and the rank of the matrix is an intrinsic parameter that conserves in the elementary transformations.